Published OnlineFirst December 6, 2017; DOI: 10.1158/0008-5472.CAN-17-1720

Priority Report

Cancer Research

T-Cell Densities in Brain Metastases Are Associated with Patient Survival Times and Diffusion Tensor MRI Changes

Rasheed Zakaria[1,2], Angela Platt-Higgins[2], Nitika Rathi[3], Mark Radon[4], Sumit Das[3], Kumar Das[4], Maneesh Bhojak[4], Andrew Brodbelt[1], Emmanuel Chavredakis[1], Michael D. Jenkinson[1,5], and Philip S. Rudland[2]

Abstract

Brain metastases are common and are usually detected by MRI. Diffusion tensor imaging (DTI) is a derivative MRI technique that can detect disruption of white matter tracts in the brain. We have matched preoperative DTI with image-guided sampling of the brain–tumor interface in 26 patients during resection of a brain metastasis and assessed mean diffusivity and fractional anisotropy (FA). The tissue samples were analyzed for vascularity, inflammatory cell infiltration, growth pattern, and tumor expression of proteins associated with growth or local invasion such as Ki67, S100A4, and MMP2, 9, and 13. A lower FA in the peritumoral region indicated more white matter tract disruption and independently predicted longer overall survival times (HR for death = 0.21; 95% confidence interval, 0.06–0.82; $P = 0.024$). Of all the biological markers studied, only increased density of $CD3^+$ lymphocytes in the same region correlated with decreased FA (Mann–Whitney U, $P = 0.037$) as well as confounding completely the effect of FA on multivariate survival analyses. We conclude that the T-cell response to brain metastases is not a surrogate of local tumor invasion, primary cancer type, or aggressive phenotype and is associated with patient survival time regardless of these biological factors. Furthermore, it can be assayed by DTI, potentially offering a quick, noninvasive, clinically available method to detect an active immune microenvironment and, in principle, to measure susceptibility to immunotherapy.

Significance: These findings show that white matter tract integrity is degraded in areas where T-cell infiltration is highest, providing a noninvasive method to identify immunologically active microenvironments in secondary brain tumors. *Cancer Res; 78(3); 610–6. ©2017 AACR.*

Introduction

Brain metastasis (BM) is a profound clinical problem, causing significant morbidity and mortality in patients with solid organ cancers; however, they are poorly responsive to traditional chemotherapeutic agents. There has been little investigation of the interface between the brain and the brain metastasis (B-BM) in patients undergoing treatment; however, there are now strong reasons for doing so (1–3). First, it has recently been shown that far from being discrete and encapsulated, BMs show a variety of growth patterns at the leading edge, with implications for prognosis and treatment (1, 4). Second, the B-BM interface is the region in which the tumor interacts with the host immune system (5, 6). Third, there are new treatments that act at the B-BM interface: cavity boost radiosurgery in radiation oncology, immune-modulating agents in medical oncology, and supramarginal resection in neurosurgery (7, 8).

MRI provides a quick, widely available modality to assess the B-BM interface noninvasively and can deliver information that applies to both resected and nonresected tumors. Diffusion along white matter tracts in the brain assessed by MRI is particularly sensitive at detecting changes at the B-BM interface (9, 10), although MR spectroscopy (for tumor metabolism, cellular proliferation) and MR perfusion (for increased blood flow) may also detect changes not seen on conventional imaging. Disruption of white matter tracts causes reduced fractional anisotropy (FA) without necessarily reducing mean diffusivity (MD), and this may indicate local tumor invasion—as has been demonstrated by meta-analysis in glioma (11, 12)—and/or other processes, such as inflammation or neoangiogenesis. Diffusion MRI has the further advantage of being quick to obtain, relatively easy to post process and reproducible across different scanners or institutions (13).

We have performed matched diffusion MRI (measuring FA and MD) with image-guided sampling of the B-BM interface for newly diagnosed patients undergoing surgery to assess MRI features, cellularity, growth pattern, cell invasion/division, and host inflammatory responses for BMs from different primary cancers in an attempt to relate them to the MRI data and patient outcomes.

[1]Department of Neurosurgery, The Walton Centre NHS Foundation Trust, Liverpool, United Kingdom. [2]Institute of Integrative Biology, University of Liverpool, Liverpool, United Kingdom. [3]Department of Neuropathology, The Walton Centre NHS Foundation Trust, Liverpool, United Kingdom. [4]Department of Neuroradiology, The Walton Centre NHS Foundation Trust, Liverpool, United Kingdom. [5]Institute of Translational Medicine, University of Liverpool, Liverpool, United Kingdom.

Note: Supplementary data for this article are available at Cancer Research Online (http://cancerres.aacrjournals.org/).

Corresponding Author: Rasheed Zakaria, University of Liverpool, Biosciences Building, Crown Street, Liverpool L69 7ZB, United Kingdom. Phone: 441515295945; Fax: 441517942000; E-mail: rzakaria@nhs.net

doi: 10.1158/0008-5472.CAN-17-1720

Published OnlineFirst December 6, 2017; DOI: 10.1158/0008-5472.CAN-17-1720

Table 1. Clinical features of patients studied

Characteristic	Number	% of total
Age at surgery/years (range)	62.9	(23.8–76.0)
Gender		
Female	14	53.8%
Male	12	46.2%
Karnofsky performance score		
80	5	19.2%
90	18	69.2%
100	3	11.5%
Primary cancer		
Non–small cell lung	13	50%
Breast	4	15.4%
Melanoma	4	15.4%
Colorectal	2	7.7%
Renal	1	3.8%
Other	2	7.7%
Extracranial metastases		
Absent	18	69.2%
Present	8	30.8%
Control of primary disease		
Synchronous	9	34.6%
Controlled	17	65.4%
Adjuvant WBRT (30 Gy in 10#)		
No	5	19.2%
Yes	21	80.8%
Adjuvant chemotherapy		
None	13	50.0%
Yes	9	34.6%
Targeted agent	4	15.4%
OS/months (range)	5.8	(1.6–15.5)
Intracranial progression		
None	16	61.5%
Local	7	26.9%
Distant	3	11.5%
Progression-free survival/months (range)	3.8	(0.2–12.9)

Patients and Methods

Patients and follow-up

Overall 26 patients were studied prospectively, and the clinical details are summarized in Table 1. Patient study was conducted in accordance with the principles of the Declaration of Helsinki. Ethical approval was granted as an internal project within the institution's Research Tissue Bank after board review (National Research Ethics Service ID 11/WNo03/2), and patients provided written informed consent for inclusion in this bank before surgery. All patients underwent complete resection of a symptomatic, supratentorial BM in the course of routine clinical care (including dexamethasone 16 mg per day in divided doses for at least 72 hours prior to surgery) at a single institution. Postoperative clinical course and care including radiotherapy or the use of adjuvant systemic chemotherapy (including targeted agents) were recorded prospectively, as these were potential confounding factors for survival. Intracranial progression was determined by a neuroradiologist as per standard criteria (14) in combination with the clinical findings, and all patients were discussed at the interdisciplinary tumor board.

MRI studies and image-guided sampling

At a median of 5 days prior to surgery, patients underwent an MRI brain scan protocoled by a clinical neuroradiologist, and further details of sequences are provided in Supplementary Methods but are summarized here. A volumetric fast spoiled gradient echo sequence was taken after gadolinium injection at a standard dose of 0.1 mmol/kg (repetition time/echo time, 9/1.4 ms; flip angle, 15°; acquisition matrix, 256 × 256; volume, 180 × 1 mm^2 slices at zero angle gantry); this is referred to as the planning scan. Scans were reviewed by a clinical neuroradiologist including scoring the degree of edema on T2 weighted using a previously defined scale (15). Following standard postprocessing (e.g., to correct for eddy current distortion), maps of FA and MD were generated using DTIstudio, version 3.0.3 (16). In theatre, the planning scan was used for registration to a neuronavigation system (StealthStation S7, Medtronic Inc.). For each case, a biopsy location was chosen that showed a radiologic and histologic interface with brain. In the course of tumor resection, patients had image-guided samples taken from this location using standard forceps with a tracking device attached, so that the real-time location of the forceps tip could be followed. These forceps yielded specimens of approximately 4 × 3 × 2 mm^3, and the location was electronically marked on the planning scan as samples were taken (17).

After surgery, the vector specifying this location was extracted from the image guidance software and transferred offline to the image analysis software. Each location was double-checked visually with screenshots taken in three orthogonal planes at the biopsy location during surgery. A region of interest (ROI) placed at this location in the image analysis software, which was colocalized to the tissue sample taken intraoperatively, could then be applied to the MRI parametric maps generated as these maps were also coregistered to the planning scan. Average and minimum readings of MD and FA were taken on the tumor and brain side of the B-BM interface at the biopsy location for each case. Control readings were taken from the contralateral white matter by flipping the ROIs across the anatomical midline, ensuring that this avoided any confounding structures such as ventricles or bone.

Tissue analysis

Histologic assessment by a neuropathologist was performed to determine the primary cancer of origin, confirm the diagnosis of metastasis, and categorize the growth pattern (4). A number of proteins acting as markers of proliferation (Ki67), glial cells (GFAP), inflammatory cells (CD3, CD8, CD4, CD20, CD68, FOXP3, PD1), connective tissue (reticulin, CD34), ECM adhesion/remodeling (MMP 2,9,13), and metastasis (S100A4, S100P, AGR2, OPN) were examined by immunohistochemistry and manually and electronically scored for how intense and widespread the staining was using validated methods (18). Absolute numbers of immunoreactive lymphocytes and macrophages were manually counted per high-powered field (HPF); further detail on the methods as well as how biopsy samples were processed and the types and serial numbers of commercially available antibodies are provided online in Supplementary Methods.

Statistical methods

Overall survival (OS) was taken as the time from surgery to death; a noncancer death or those lost to follow up were censored at the last recorded follow-up. Patients who died before progression were censored at the last date of follow-up imaging. Significant differences were assessed using the Fisher two-sided exact test. Time-to-event comparisons were made using the Kaplan–Meier method with log-rank tests and

Published OnlineFirst December 6, 2017; DOI: 10.1158/0008-5472.CAN-17-1720

multivariate analyses conducted using the Cox method. Correlations were assessed using Spearman Rank Test and pairwise comparisons using Wilcoxon-signed rank test. Data processing was performed using SPSS version 22.0 (IBM) and R version 3.10 (R Core Team, 2013).

Results

Clinical outcomes

Postoperative CT brain scan within 24 hours confirmed complete resection of the contrast-enhancing lesion, and there were no postoperative complications such as infection or hematoma. Median OS was 5.5 months [95% confidence interval (CI), 4.2–6.8]. The only factors associated with increased OS were tumor size (median, 8.2 months < 30 mm diameter vs. 5.2 months if larger, log-rank 5.65, $P = 0.017$) and administration of postoperative whole brain radiotherapy (WBRT; median, 6.5 months vs. 2.7 months untreated, log-rank 16.26, $P < 0.001$).

MRI suggests two different prognostic phenotypes, unrelated to biological features of the tumor

The median FA readings in the peritumoral region where tissue was obtained from were consistently lower than control white matter from the comparable brain region in the unaffected, contralateral hemisphere [0.140; interquartile range (IQR), 0.106–0.176 vs. 0.198; IQR, 0.162–0.235, matched samples Wilcoxon-signed rank test, $P < 0.001$). We observed two populations within the group, as illustrated in Fig. 1A–F. Those cases with a low peritumoral FA (<median) showed significantly longer survival times (median, 9.9 months; 95% CI, 7.4–12.4 vs. 5.3 months; 95% CI, 3.4–7.13, log-rank = 4.57, $P = 0.033$), Fig. 1G and H, even when confounding variables were introduced (Cox's multivariate analysis: Table 2A and B; HR for death = 0.21; 95% CI, 0.06–0.82, $P = 0.024$). The colocalized samples obtained at the B-BM interface were analyzed in relation to the different MRI phenotypes (high FA vs. low FA). The primary cancer type and metastasis growth pattern (diffuse vs. encapsulated) as assessed by a neuropathologist (4) did not show any association with FA readings at the leading edge of the tumor or in the adjacent peritumoral region. There was no difference in the tumor expression of relevant matrix metalloproteinases (MMP 2, 9, and 13), tumor cellularity, Ki67 proliferative index, tumor or peritumoral vascularity (assessed as CD34-positive blood vessel density), necrosis, or connective tissue density (reticulin and GFAP staining) between the high and low FA cases.

Local cellular immune response is heterogeneous and unrelated to biological features of the tumor

Assessment of the cellular immune response at the B-BM interface revealed a dense CD68-positive macrophage infiltration compared with the metastasis core—median, 62 cells per HPF, IQR, 43–105 in peritumoral regions vs. 21 cells/HPF (IQR, 13–33) in control white matter; these cells formed a band surrounding the tumor rather than focal islands or a diffuse infiltrate extending away from the tumor edge. In contrast, T-cell (CD3-positive lymphocyte) infiltration was heterogeneous (Fig. 1B, C, E, F and Fig. 2A). Although consistently present in the peritumoral region (median 16 cells/HPF, significantly greater than control white matter, Mann–Whitney *U*, $P < 0.001$), the density of T cells varied from 0 to 113 cells/HPF. This was neither a function of the primary cancer type nor of any clinical features tested, e.g., control of the primary cancer, presence of extracranial metastases, intracranial location, growth pattern, markers of aggressive growth/invasion, or patient age (all comparisons nonsignificant by the Kruskal–Wallis test). Low B-cell (CD20-positive) infiltration was observed in all regions (Fig. 2A).

Peritumoral T-cell infiltrates were further stained for CD4, CD8, FOX-P3, and PD-1 (Fig. 2B). Mean ratio of cytotoxic ($CD8^+$) to helper ($CD4^+$) cells in the peritumoral region was 1.5:1, with no significant difference observed by primary cancer or any other biological factor relating to the metastasis or the patient (Kruskal–Wallis and Friedman's Analysis of Variance by ranks tests). The percentage of regulatory, FOX-P3–positive T cells varied from 34% in the core to 24% at the leading edge and 16% in the peritumoral region, with a lower density of FOX-P3–positive cells in those BMs with extracranial metastases (Mann–Whitney *U*, $P = 0.001$) and those presenting with a previously treated primary cancer (Mann–Whitney *U*, $P = 0.012$). Regarding possible susceptibility to existing immunotherapy drugs, 52% of T cells in the peritumoral region were PD-1 receptor positive (compared with 15% in core and 25% at leading edge), and the proportion of T cells that were PD-1 positive was no greater around or in those BMs expressing PD-L1. PD-L1 staining was detected in 13 of 26 tumors studied with no relation to the primary cancer or the levels of immune cells seen and no effect on patient survival in this series.

Peritumoral T cells are associated with low FA and prolonged patient survival

The peritumoral density of $CD3^+$ T cells was the only significant biological difference observed between the high and low FA groups (Mann–Whitney *U*, $P = 0.037$); there were no differences in the presence of other immunoreactive cells in the same region (macrophages, $P = 0.867$; B cells, $P = 0.074$; all immune cells combined, $P = 0.232$) nor in vascularity ($CD34^+$ blood vessels, $P = 0.673$). The continuous values for peritumoral T-cell density and peritumoral FA were compared with matched samples, and these correlated strongly (Spearman rho = −0.676, $P = 0.003$), whereas there was no significant correlation with other MRI features such as the degree of T2 edema (0.233, $P = 0.262$). There was no difference in the MD in those cases with high versus low peritumoral T-cell infiltration (median samples test $P = 0.684$) and no correlation of the MD with T-cell density (Spearman 0.113, $P = 0.599$).

The differential response in different BMs is clinically relevant, because increased peritumoral $CD3^+$ T-cell density was significantly associated with prolonged survival time (median, 8.1 months vs. 5.2 months; log-rank 5.77, $P = 0.016$; Fig. 2C, Table 2B–D). When further categorized into 3 groups (<5, 5–25, and >25 immunoreactive cells per high power field), those patients with moderate peritumoral $CD3^+$ T-cell infiltration appeared to be at no advantage compared with those with low infiltration, whereas those with the highest infiltration lived over twice as long [median, 11.7 months vs. 5.1, 5.2 months for moderate and low groups, respectively, log-rank (pooled) = 10.06, 2 d.f., $P = 0.007$; Figs. 1G and 2D). A number of important biological factors were excluded as potential confounders including macrophage, B-cell, T-cell subtypes (CD4/8/FOX-P3/PD-1), growth pattern (invasive or pseudo-encapsulated), metalloproteinases (MMP 2, 9, 13) or metastasis-inducing proteins (19), cellularity, Ki67 proliferative index, vascularity, necrosis, connective tissue density at the leading edge, and clinical factors, such as extracranial metastases,

Published OnlineFirst December 6, 2017; DOI: 10.1158/0008-5472.CAN-17-1720

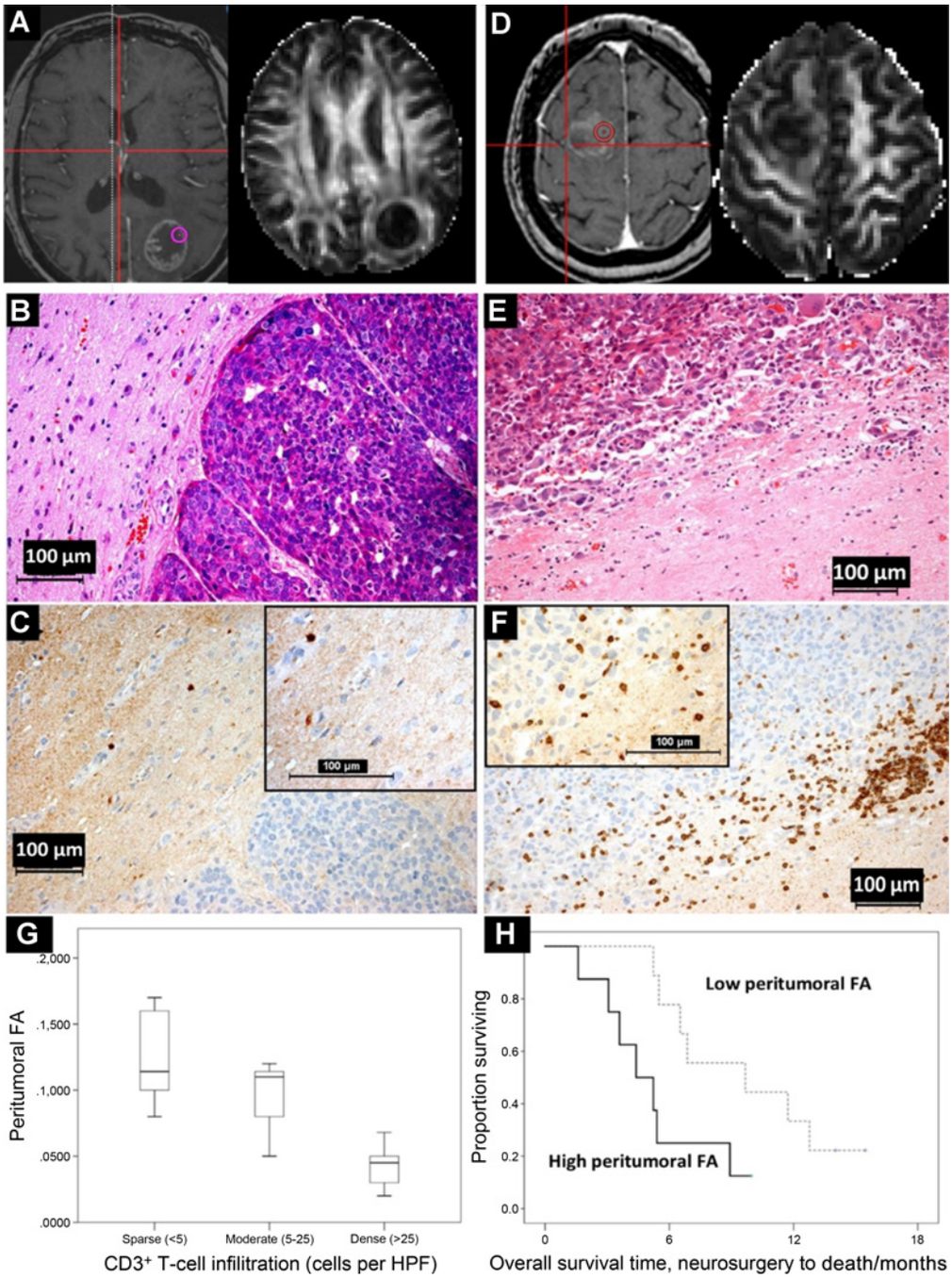

Figure 1.

Two different populations of BMs identified by DTI. **A,** Lung adenocarcinoma metastasis that shows little white matter disruption and has a high peritumoral FA value at the biopsy location shown. **B,** Hematoxylin and eosin of biopsy. **C,** CD3-stained serial section showing sparse T-cell infiltration in the same region (inset magnified). **D,** In contrast, a breast cancer metastasis shows more visible white matter change and the FA value in the peritumoral region shown is lower. **E,** Hematoxylin and eosin. **F,** CD3-stained section of biopsy. Here, there is dense peritumoral T-cell infiltration (inset, magnified). **G,** Values of FA-differentiated categories of peritumoral $CD3^+$ T-cell density in the colocalized image-guided biopsy regions, and the differences are significant (Kruskal–Wallis, $P = 0.033$). **H,** Cases with high peritumoral FA (>median) died significantly sooner after neurosurgical resection of their metastasis than those with a low peritumoral FA (9.9 months vs. 5.3 months, log-rank statistic = 4.566, $P = 0.033$).

primary cancer, age, and performance status. However, when both low FA and high peritumoral levels of T cells were included in Cox's multivariate analysis either alone (Table 2A and B) or with the other potentially confounding variables (Table 2D), high peritumoral T-cell density completely confounds low peritumoral FA in its association with patient survival times so rendering the

Published OnlineFirst December 6, 2017; DOI: 10.1158/0008-5472.CAN-17-1720

Table 2. Multivariate Cox proportional hazards model for OS

	HR for death	95% CI for HR	Sig.
A			
Adjuvant whole brain radiotherapy given	0.08	0.01–0.51	0.008[a]
Tumor size: longest axis > 30 mm	2.80	0.85–9.25	0.091
Low peritumoral FA (more white matter tract disruption)	0.21	0.06–0.82	0.024[a]
B			
Adjuvant whole brain radiotherapy given	0.10	0.03—0.39	0.001[a]
Tumor size: longest axis > 30 mm	3.37	1.29—8.81	0.013[a]
High peritumoral density of $CD3^+$ T cells	0.40	0.13—1.25	0.114
C			
Low peritumoral FA (more white matter tract disruption)	0.96	0.26–4.19	0.964
High peritumoral density of $CD3^+$ T cells	0.08	0.12–0.49	0.007[a]
D			
Adjuvant whole brain radiotherapy given	0.29	0.04–2.33	0.242
Tumor size: longest axis > 30 mm	3.11	0.87–11.18	0.082
High peritumoral density of $CD3^+$ T cells	0.09	0.01–1.13	0.062
Low peritumoral FA (more white matter tract disruption)	0.83	0.11–6.58	0.862

NOTE: Models incorporating: **A,** All factors that were significant at univariate log-rank analysis. **B,** All factors significant at univariate analysis but with T-cell density substituted for peritumoral FA. **C,** Only FA and peritumoral T-cell infiltration, which confound one another. **D,** All factors significant at univariate analysis including both FA and peritumoral T-cell density.
[a]$P < 0.05$.

contribution from FA completely insignificant (Table 2C). This result suggests that both are a reflection of the same or associated phenomenon irrespective of the other variables.

Discussion

Because the nature of samples obtained in this study is not routinely available in clinical practice unless intentionally

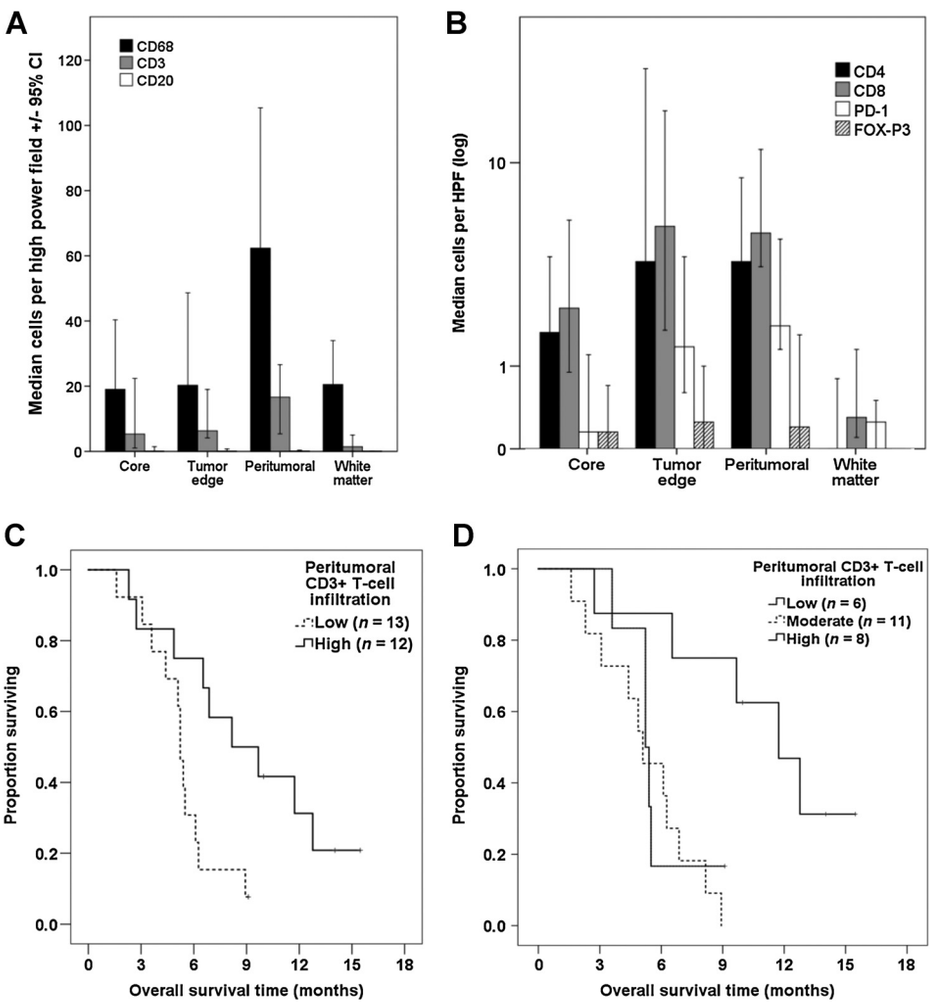

Figure 2.
Cellular-immune reaction to BMs. Absolute numbers of immunoreactive cells/HPF were counted in specimens obtained from image-guided resection of BMs. **A,** Highest infiltrates were present in the peritumoral region for both $CD68^+$ macrophages (median, 62 cells/HPF; 95% CI, 45–105) and $CD3^+$ T cells (median, 16 cells/HPF; 95% CI, 6–25) while few or no $CD20^+$ B cells were seen (median, 0 cells/HPF; 95% CI, 0.1–1.1). **B,** T cells seen were a mixture of $CD8^+$ effector cells and $CD4^+$ helper cells, with PD-1 receptor–positive and regulatory FOX-P3–positive cells occurring predominantly at the tumor edge and peritumoral region. **C,** High peritumoral T-cell count (>16 cells per HPF) was associated with improved OS times for resected BMs, compared with lower than median count (<16 cells per HPF; log-rank test = 5.77, $P = 0.016$). **D,** Highest peritumoral T-cell counts (>25 per HPF) were associated with longer OS times compared with moderate (5–25) and low (<5) T-cell counts (log-rank statistics = 10.15 and 4.84 and $P =$ 0.001 and 0.028, respectively). There was no significant difference between moderate and low T-cell counts (log-rank 0.242, $P = 0.623$).

Published OnlineFirst December 6, 2017; DOI: 10.1158/0008-5472.CAN-17-1720

performing a supramarginal resection (7, 8), this is the first *in vivo* examination of the relationship between white matter disruption and inflammation for BMs. Here, we have shown for the first time that the FA in the peritumoral region is closely associated with the density of $CD3^+$ T-cell infiltration but the MD is not. Both increased T-cell infiltration and reduced FA (corresponding to more white matter tract disruption) are associated with prolonged OS time after resection of the metastasis, and one parameter completely confounds the other in this respect. Because all the imaging and biological data are obtained from the same region using image-guided surgical procedures, we suggest that FA in the peritumoral region is possibly acting as a surrogate marker of the immune response to the BM. This is a novel finding that further supports the existing evidence for the tumor microenvironment in mediating BM behavior and adds the possibility of assaying this inflammatory response noninvasively in patients with different primary cancers, in a clinically relevant context, using a widely available and studied imaging technique.

The MRI characteristics of BMs have been extensively studied previously using diffusion weighted imaging and diffusion tensor imaging (DTI), and readings obtained in our series are entirely in keeping with those previously recorded, although not their interpretation. Even those studies that focused on the B-BM interface by measuring changes in the peritumoral region have focused exclusively on invasion (11, 12). However, the brain is uniquely sensitive to inflammatory changes, and hence white matter disruption, assessed by changes in anisotropic diffusion, has been shown in a variety of pathologies in large numbers (20). In contrast to glioma, BMs do not diffusely infiltrate the brain; therefore, the change in white matter signal may have a different cause than simple invasion. Because the central nervous system is an immune-privileged environment, the DTI changes may be inflammatory, as suggested by postmortem (21), animal (10), and now *in vivo* human study.

Our patient group is not unusual except that traditional predictive factors such as age and performance status—which are incorporated in scoring systems (22)—were not significant for survival. However, all the patients selected for neurosurgical intervention would tend to be of high performance status and younger age in any case, explaining this finding. The image guidance system used is of the sort routinely used in clinical neurosurgical practice in Europe and North America, and localization accuracy is dependent on a number of factors from the fidelity of the planning MRI to the image registration algorithms. Accuracy could potentially be improved by using rigid frame-based neuronavigation or a robot-mounted tool to take samples as opposed to a hand-held forceps, but this would limit the angle of sampling and ability to maneuver the probe to the true B-BM interface under direct vision and navigation. Finally, in neuronavigation, there is an issue of brain shift where the preregistered navigation loses some accuracy once the dura is opened and CSF is released. Although this can be corrected for potential inaccuracy using intraoperative ultrasound, this procedure is not routine clinical practice as it requires intense computational power and incurs a time delay, for little benefit in accuracy when dealing with mostly superficial tumors (metastases are usually seen at the gray-white matter zone), where underlying brain edema often balances the loss of CSF on opening the dura.

Immune response and in particular quantifying tumor-associated $CD3^+$ T cells are currently of great interest as a means of improving prognostication and developing therapies in cancer medicine. A small number of descriptions have disagreed on the *degree* of T-cell infiltration in BMs from solid organ cancers (5, 23). Here, we show there is considerable variation in inflammatory cells with location, and this does not depend on the primary tumor type or the growth pattern of the BM; this is important in studying the biology of these tumors, given recent study has suggested that there may be more and less locally invasive subtypes (1). Furthermore, proteins known to be involved in local invasion and recently found to be highly associated with local recurrence and overexpressed at the BM leading edge (19) do not appear to modulate the local cellular immune response, nor did the BM expression of PD-L1. The latter result suggests more caution is needed if PD-L1 expression is to be taken as the sole marker of susceptibility to immune-modulating therapies in some primary types (e.g., melanoma; ref. 5).

There is an urgent need for better biomarkers of susceptibility to immunotherapy. These treatments, although potentially huge in their impact on survival for patients with metastatic disease, are only effective in some cases (perhaps 20%–50% depending on estimates), and they have considerable costs, both financial and in terms of potentially harmful side effects. There remain no standard criteria for predicting tumor response, and responses are difficult to distinguish during tumor growth using conventional imaging, although reports using other modalities are emerging (24). Diffusion MRI is a well-established technique with huge numbers of reports on the theoretical basis and practical application in neuro-oncology imaging. It is therefore highly important if this technique could be repurposed to predict in advance of obtaining tissue (often not performed for BM patients with an established primary cancer) whether there is an "immune active" microenvironment in this case T-cell infiltration, which is known to be a predictor of response to immunotherapy (25). Further longitudinal study with imaging at multiple time points or after immunotherapy would be important in validating this finding, although repeat, corroborative tissue sampling from peritumoral brain is unlikely to be obtained in the future.

In conclusion, we have tested and excluded the hypothesis that the immune reaction to BMs depends on tumor factors such as primary cancer type, growth pattern, and expression of proteins mediating local invasion and recurrence. We have shown instead that the $CD3^+$ T-cell density in the peritumoral region is the only biological factor independently associated with OS for patients with an operated BM from solid organ cancers. Higher T-cell infiltration in this region colocalizes with white matter disruption and a decrease in anisotropic diffusion as measured noninvasively by DTI. Because the immune response is a marker of susceptibility to immune-modifying drugs and most patients with BMs are not suitable for resection and hence tissue biomarkers, this is therefore a routinely available clinical technique that could in future be used as part of the work up before considering immunotherapy.

Disclosure of Potential Conflicts of Interest

No potential conflicts of interest were disclosed.

Authors' Contributions

Conception and design: R. Zakaria, M. Bhojak, M.D. Jenkinson, P.S. Rudland
Development of methodology: R. Zakaria, A. Platt-Higgins, M. Bhojak
Acquisition of data (provided animals, acquired and managed patients, provided facilities, etc.): R. Zakaria, A. Platt-Higgins, N. Rathi, K. Das, M. Bhojak, A. Brodbelt, E. Chavredakis, M.D. Jenkinson, P.S. Rudland

Analysis and interpretation of data (e.g., statistical analysis, biostatistics, computational analysis): R. Zakaria, S. Das, K. Das, M.D. Jenkinson, P.S. Rudland
Writing, review, and/or revision of the manuscript: R. Zakaria, A. Platt-Higgins, M. Radon, S. Das, K. Das, M. Bhojak, A. Brodbelt, M.D. Jenkinson, P.S. Rudland
Administrative, technical, or material support (i.e., reporting or organizing data, constructing databases): A. Platt-Higgins, S. Das
Study supervision: M.D. Jenkinson, P.S. Rudland

Acknowledgments

R. Zakaria received support from The Medical Research Council (MRC) UK - grant MR/L017342/1 and the Royal College of Surgeons of England (RCS) via a Research Training Fellowship. P.S. Rudland received support from the Cancer and Polio Research Fund, UK and MRC (UK) - grant G0801447.

We thank Khaja Syed of The Walton Centre NHS Foundation Trust for his assistance with tissue banking. This work has been presented at the EORTC Brainmets conference 2016 and the AACR Tumor Immunotherapy and Immunology Meeting 2016 and is being published as an abstract in the proceedings of those meetings.

The costs of publication of this article were defrayed in part by the payment of page charges. This article must therefore be hereby marked *advertisement* in accordance with 18 U.S.C. Section 1734 solely to indicate this fact.

Received June 21, 2017; revised September 15, 2017; accepted November 21, 2017; published OnlineFirst December 6, 2017.

References

1. Siam L, Bleckmann A, Chaung HN, Mohr A, Klemm F, Barrantes-Freer A, et al. The metastatic infiltration at the metastasis/brain parenchyma-interface is very heterogeneous and has a significant impact on survival in a prospective study. Oncotarget 2015;6:29254–67.
2. Raore B, Schniederjan M, Prabhu R, Brat DJ, Shu HK, Olson JJ. Metastasis infiltration: an investigation of the postoperative brain-tumor interface. Int J Rad Oncol Biol Phys 2011;81:1075–80.
3. Baumert BG, Rutten I, Dehing-Oberije C, Twijnstra A, Dirx MJ, Debougnoux-Huppertz RM, et al. A pathology-based substrate for target definition in radiosurgery of brain metastases. Int J Rad Oncol Biol Phys 2006;66:187–94.
4. Berghoff AS, Rajky O, Winkler F, Bartsch R, Furtner J, Hainfellner JA, et al. Invasion patterns in brain metastases of solid cancers. Neuro Oncol 2013;15:1664–72.
5. Kluger HM, Zito CR, Barr ML, Baine MK, Chiang VL, Sznol M, et al. Characterization of PD-L1 expression and associated T-cell infiltrates in metastatic melanoma samples from variable anatomic sites. Clin Cancer Res 2015;21:3052–60.
6. Sugihara AQ, Rolle CE, Lesniak MS. Regulatory T cells actively infiltrate metastatic brain tumors. Int J Oncol 2009;34:1533–40.
7. Yoo H, Kim YZ, Nam BH, Shin SH, Yang HS, Lee JS, et al. Reduced local recurrence of a single brain metastasis through microscopic total resection. J Neurosurg 2009;110:730–6.
8. Kamp MA, Rapp M, Slotty PJ, Turowski B, Sadat H, Smuga M, et al. Incidence of local in-brain progression after supramarginal resection of cerebral metastases. Acta Neurochir 2015;157:905–10; discussion 10–1.
9. Zakaria R, Das K, Radon M, Bhojak M, Rudland PR, Sluming V, et al. Diffusion-weighted MRI characteristics of the cerebral metastasis to brain boundary predicts patient outcomes. BMC Med Imaging 2014;14:26.
10. Serres S, Martin CJ, Sarmiento Soto M, Bristow C, O'Brien ER, Connell JJ, et al. Structural and functional effects of metastases in rat brain determined by multimodal MRI. Int J Cancer 2014;134:885–96.
11. Lemercier P, Paz Maya S, Patrie JT, Flors L, Leiva-Salinas C. Gradient of apparent diffusion coefficient values in peritumoral edema helps in differentiation of glioblastoma from solitary metastatic lesions. Am J Roentgenol 2014;203:163–9.
12. Jiang R, Du FZ, He C, Gu M, Ke ZW, Li JH. The value of diffusion tensor imaging in differentiating high-grade gliomas from brain metastases: a systematic review and meta-analysis. PLoS One 2014;9:e112550.
13. Grech-Sollars M, Hales PW, Miyazaki K, Raschke F, Rodriguez D, Wilson M, et al. Multi-centre reproducibility of diffusion MRI parameters for clinical sequences in the brain. NMR Biomed 2015;28:468–85.
14. Lin NU, Lee EQ, Aoyama H, Barani IJ, Barboriak DP, Baumert BG, et al. Response assessment criteria for brain metastases: proposal from the RANO group. Lancet Oncol 2015;16:e270–8.
15. Spanberger T, Berghoff AS, Dinhof C, Ilhan-Mutlu A, Magerle M, Hutterer M, et al. Extent of peritumoral brain edema correlates with prognosis, tumoral growth pattern, HIF1a expression and angiogenic activity in patients with single brain metastases. Clin Exp Metast 2013;30:357–68.
16. Jiang H, van Zijl PC, Kim J, Pearlson GD, Mori S. DtiStudio: resource program for diffusion tensor computation and fiber bundle tracking. Comput Methods Programs Biomed 2006;81:106–16.
17. Zakaria R, Jenkinson MD. Using ADC maps with structural scans to improve intraoperative biopsy specimens in brain metastases. Neuroradiol J 2014;27:422–4.
18. Rudland PS, Platt-Higgins A, Renshaw C, West CR, Winstanley JH, Robertson L, et al. Prognostic significance of the metastasis-inducing protein S100A4 (p9Ka) in human breast cancer. Cancer Res 2000;60:1595–603.
19. Zakaria R, Platt-Higgins A, Rathi N, Crooks D, Brodbelt A, Chavredakis E, et al. Metastasis-inducing proteins are widely expressed in human brain metastases and associated with intracranial progression and radiation response. Br J Cancer 2016;114:1101–8.
20. Jiang Q, Zhang ZG, Chopp M. MRI evaluation of white matter recovery after brain injury. Stroke 2010;41:S112–3.
21. Berghoff AS, Lassmann H, Preusser M, Hoftberger R. Characterization of the inflammatory response to solid cancer metastases in the human brain. Clin Exp Metast 2013;30:69–81.
22. Sperduto PW, Kased N, Roberge D, Xu Z, Shanley R, Luo X, et al. Summary report on the graded prognostic assessment: an accurate and facile diagnosis-specific tool to estimate survival for patients with brain metastases. J Clin Oncol 2012;30.
23. Berghoff AS, Ricken G, Widhalm G, Rajky O, Dieckmann K, Birner P, et al. Tumour-infiltrating lymphocytes and expression of programmed death ligand 1 (PD-L1) in melanoma brain metastases. Histopathology 2015;66:289–99.
24. Larimer BM, Wehrenberg-Klee E, Caraballo A, Mahmood U. Quantitative CD3 PET imaging predicts tumor growth response to anti-CTLA-4 therapy. J Nucl Med 2016;57:1607–11.
25. Gnjatic S, Bronte V, Brunet LR, Butler MO, Disis ML, Galon J, et al. Identifying baseline immune-related biomarkers to predict clinical outcome of immunotherapy. J Immunother Cancer 2017;5:44.

Cancer Research
The Journal of Cancer Research (1916–1930) | The American Journal of Cancer (1931–1940)

AACR American Association for Cancer Research

T-Cell Densities in Brain Metastases Are Associated with Patient Survival Times and Diffusion Tensor MRI Changes

Rasheed Zakaria, Angela Platt-Higgins, Nitika Rathi, et al.

Cancer Res 2018;78:610-616. Published OnlineFirst December 6, 2017.